Research article

Electromagnetic radiation and electrical stimulation controls of absence seizures in a coupled reduced corticothalamic model

Xiaolong Tan, Hudong Zhang, Yan Xie and Yuan Chai*

School of Mathematics and Physics, Shanghai University of Electric Power, Shanghai 201306, China

* Correspondence: Email: chaiyuan@shiep.edu.cn.

Abstract: The important role of basal ganglia in corticothalamic loops has received widespread attention. However, its connection between coupled reduced corticothalamic networks is rarely researched, particularly the regulatory mechanism about electromagnetic radiation and electrical stimulation has not been comprehensively investigated. In this paper, we establish a model simplified the basal-ganglia as a connector connecting two corticothalamic loops. Four kinds of treatment methods are applied to the coupled reduced corticothalamic model, for instance deep brain stimulation (DBS), 1:0 coordinate reset stimulation (CRS) and 3:2 CRS to stimulate thalamic reticular nucleus (TRN) and electromagnetic radiation to stimulate the pyramidal neuronal population (PY). One of the important results is that the epileptic area can be significantly reduced in varying degrees by changing the strength of the basal-ganglia connector. Another one is that electromagnetic radiation, DBS and CRS have preferable inhibitory effects on absence seizure. The results show that DBS has a more significant inhibitory effect than 1:0 CRS and 3:2 CRS. The results might contribute to understanding the role of basal ganglia in coupled model and providing a reference for inhibiting epileptic seizures.

Keywords: absence seizures; corticothalamic model; memristor; deep brain stimulation; coordinated reset stimulation

1. Introduction

Absence seizure, a neurological disease of the brain, often occurs in the childhood [1,2], which is characterized by a temporary loss of consciousness and bidirectional synchronous spike wave discharges (SWDs) with a frequency of 2–4 Hz recorded in an electroencephalogram (EEG) [3]. These

abnormal discharges can cause learning and cognitive problems [4–6]. Numerous studies have shown that the production of these abnormal discharges is related to the interaction between the cerebral cortex and thalamus [7–9]. Specially, the basal ganglia has already been confirmed to involve in the corticothalamic system to control epilepsy [10,11]. However, the control mechanism of the basal ganglia for epilepsy is unclear due to the complexity of the brain.

According to recent studies, thalamic reticular nucleus (TRN) is a structure of the thalamus and plays an important role in controlling electrical signals from the thalamus to the cerebral cortex [12,13]. Apart from this, TRN acts like a pacemaker to control epilepsy [14]. Some researchers have found that GABAergic (aminobutyric acid) signals released by TRN contribute to the inhibitory effect of thalamus on cerebral cortex. If these signals are disrupted, the patients will develop epilepsy in the brain [15,16]. Avanzini et al. pointed out that the oscillating activity of Ca2+ has an important effect on the generation of epilepsy [17]. Nanobashvili et al. shown that electrical discharge from TRN can cause limbic motor seizure [18]. Pantoja-Jiménez et al. demonstrated that high frequency discharge stimulation of TRN can inhibit the generation of SWDs in the corticothalamic system [19]. Clemente-Perez et al. proposed that TRN controls brain wide rhythms and seizures through electrical signs [20]. Chang et al. found that optical stimulation of TRN in mice can inhibit epilepsy [21]. However, there is still not enough theoretical basis for the control of epilepsy by TRN.

According to statistics, about one third of epileptic patients are difficult to control epilepsy through drug treatment in the world [22]. In some patients, surgical resection of the epileptic site may be a good treatment [23]. But 30–40% of adults with epilepsy are still difficult to treat [24]. Now we need an effective treatment for epilepsy patients. DBS has been applied to clinical treatment, animal brain research and theoretical models. Lehtimäki et al. reported that an epileptic patient was cured by stimulating the thalamus with DBS [25]. On the basis of the mean field model, Wang et al. demonstrated that the application of DBS in TRN can effectively inhibit epilepsy [14]. In the recent, CRS has been used to treat epilepsy as a new method of desynchronizing the firing of some abnormal neurons [26]. Fan et al. used CRS to stimulate different parts of the basal ganglia [27]. After that, the epileptic region of the whole model was reduced. However, how to select DBS and CRS to achieve the best therapeutic effect is still unclear.

In addition to the stimulation of external electrical signals can affect the activity of neurons, the change of the intracellular and extracellular ion concentration causing electromagnetic induction can also affect the activity of neurons. According to some studies, the electromagnetic induction caused by ion exchange and membrane current transmission can be described by magnetic flux [28–30]. Therefore, the external electromagnetic radiation is treated as a change in the magnetic flux in the cell, which can be simulated by a memristor [31]. Some studies have shown that memristors can be used to treat neurological diseases [32–34].

To understand the pathogenesis of epilepsy, the researchers have established the thalamocortical models. Fan et al. reduced the basal ganglia to a 2I:3O modulator [27]. The 2I:3O modulator receives two excitatory stimulation from the cerebral cortex and specific relay nuclei of thalamus (SRN) and outputs three inhibitory stimulation to the cerebral cortex, SRN and TRN. However, the above model only study a single thalamocortical model or two thalamocortical models without considering the influence of the basal ganglia. Therefore, our goal is to develop a model in which the two corticothalamic systems are connected by the basal ganglia. There are two main contributions in the paper. On the one hand, the basal ganglia is reduced to a simple and efficient connector, which receives two excitatory stimulations from the first cortical thalamic system and then outputs three inhibitory

stimulations to the second cortical thalamic system. Particularly, to explore the internal mechanism of absence epilepsy, we found that epilepsy can be suppressed without adding stimulations only by adjusting the coupling strength of TRN_1-SRN_1 and TRN_2-SRN_2 pathways or the coupling strength of the connector and the second cortical thalamic system. On the other hand, to explore the suppression of absence epilepsy by different schemes and targets, we applied DBS, 1:0 CRS, 3:2 CRS and electromagnetic radiation stimulation to the TRN_1 and cerebral cortex, respectively.

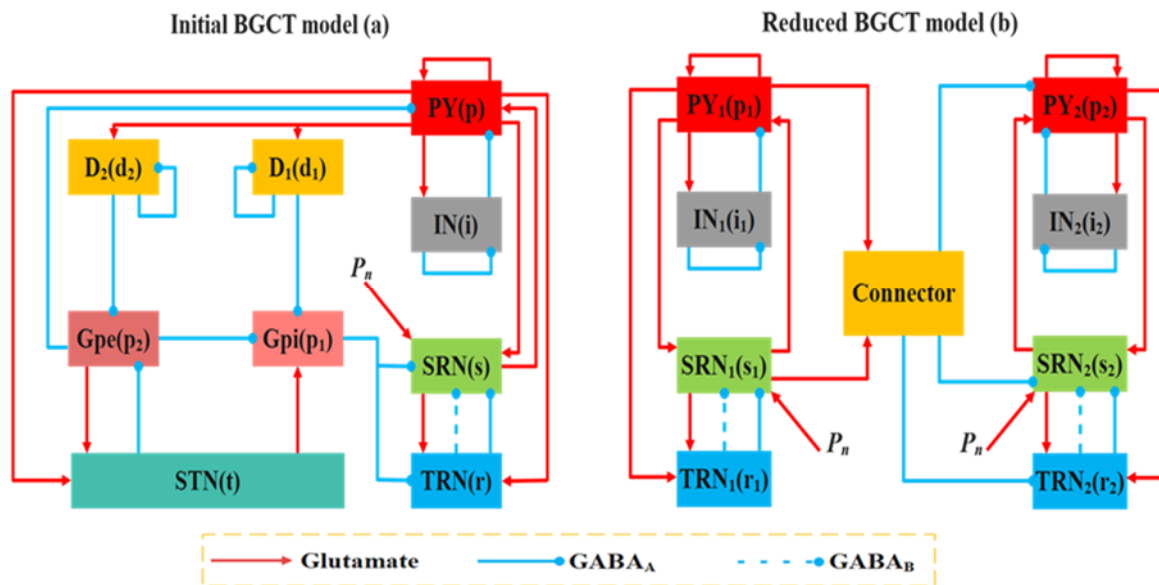## 2. The coupled reduced corticothalamic model and numerical analysis

Figure 1. Schematic drawings of initial BG-CT and coupled reduced BG-CT models: (a) The initial BG-CT model consists of three parts, i.e., cortex (PY and IN), thalamus (TRN and SRN) and basal ganglia (D_2, D_1, GPe, GPi and STN). (b) Two corticothalamic systems are connected by a connector, and the cerebral cortex and TRN of the first corticothalamic system are stimulated by electrical stimulation and electromagnetic radiation, respectively.

Chen et al. established a BGCT model as shown in Figure 1(a), which is composed of the cortical thalamic system and basal ganglia [35,36]. In this model, the cortical thalamic system is composed of two parts, cortical excitatory pyramidal neurons and inhibitory interneurons in the cortical thalamic system, thalamic relay nuclei and reticular nucleus in the thalamic system. The basal ganglia is made up of three parts: subthalamic nucleus, striatal D_1 and D_2, globus pallidus internal and external segments. In Figure 1(a), the excitatory stimulus is represented by the red arrow and is transmitted through the medium of glutamate. The soild and dashed blue lines indicate inhibitory stimulus mediators transmitted by $GABA_A$ and $GABA_B$, respectively. P_n is a nonspecific subthalamic input. Fan et al. developed a simplified BGCT model [27]. The basal ganglia is simplified as a 2I:3O modulator which receives excitatory stimulation from the PY and SNR and then outputs inhibitory stimulation to PY, SNR and TRN. To further study the mechanism of epilepsy, we developed a model of two cortical thalamic systems connected by a connector, as shown in Figure 1(b). The connector receives excitatory stimulation from the PY_1 and SRN_1 and outputs inhibitory stimulation to PY_2, SRN_2 and TRN_2.

To describe the dynamic of neuron population, some researchers have introduced a mean field model [37,38]. The mean firing rate of each neuron population can be described as a sigmoid function that contains the maximum deviation of the mean firing rate and the mean membrane potential at a given location r and time t. The function is shown below:

$$Q_a(r,t) = F[V_a(r,t)] = \frac{Q_a^{\max}}{1 + \exp\left[\dfrac{-\pi(V_a(r,t) - \theta_a)}{\sqrt{3}\sigma}\right]}, \tag{2.1}$$

where $a \in \Lambda_1 = \{p, i, d_2, d_1, p_2, p_1, t, s, r\}$ represent different population of neurons, Q_a^{max} represents the mean firing rate, θ_a and σ are the threshold variability of firing rate and standard deviation of the mean firing threshold, respectively. When the mean membrane potential V_a receives synaptic voltages from other neuron populations, the change in the mean membrane voltage can be modeled by the following formulas [39]:

$$D_{\alpha\beta}V_a(r,t) = \sum_{b\in\Lambda} C_{ab}\phi_b(r,t), \tag{2.2}$$

$$D_{\alpha\beta} = \frac{1}{\alpha\beta}\left[\frac{\partial^2}{\partial t^2} + (\alpha+\beta)\frac{\partial}{\partial t} + \alpha\beta\right], \tag{2.3}$$

where $D_{\alpha\beta}$ is the synaptic and dendritic filtering of the input signal represented by the differential operator. α and β represent the response of the cell body to the delay and rise time of the input signal. Cab denotes the coupling strength of the neuron population b to a. $\phi_b(r,t)$ is the input pulse rate form neuron population b to a. The delay parameter τ simulates the synaptic dynamics of GABAB. Due to the influence of GABAB, the mathematical expression of the network model is changed into a delay differential equation [40]. In the network model, the pulse generated by each neuron population a propagates to the next neuron population with an average conduction velocity v_a and produced a field ϕ_a. This type of propagation can be described by a decaying wave equation [41,42]:

$$\frac{1}{\gamma_a^2}\left[\frac{\partial^2}{\partial t^2} + 2\gamma_a^2\frac{\partial}{\partial t} + \gamma_a^2 - v_a^2\nabla^2\right]\phi_a(r,t) = Q_a(r,t), \tag{2.4}$$

here ∇^2 is the Laplace operator, r_a is the characteristic range of axons in neuron population a, $\gamma_a = v_a/r_a$ represents the time decay rate of the control pulse. In this model, it is generally believed that only the axons of the cortical pyramidal neuron population are long enough to produce a significant propagation effect. In other neuron population, their axons are too short to achieve the similar effect, therefore, $\phi_f = F[V_f](f \in \{p, d_1, d_2, p_1, p_2, s, r, t\})$. In addition, absence seizures are typically generalized seizures with dynamic activity throughout the brain. When considering the whole brain as a continuum and assuming that the spatial activity in this mean field model is uniformly distributed, its spatial derivative can be ignored and set $\nabla^2 = 0$. Therefore, the excitatory axon field in the cortex is ultimately defined as [38]:

$$\frac{1}{\gamma_p^2}\left[\frac{d^2}{dt^2}+2\gamma_p\frac{d}{dt}+\gamma_p^2\right]\phi_p(t)=Q_p(t), \tag{2.5}$$

where $\gamma_p=\frac{v_p}{r_p}$. At the same time, the mean membrane voltage and mean firing rate of the cortical inhibitory interneuron population i satisfy $V_i=V_p$ and $Q_i=Q_p$, respectively. This simplifies the mean field model and makes it more tractable for numerical simulation.

In the model of this paper, since the basal ganglia is simplified as a connector, the neuron population is represented as $a\in\Lambda_2=\{p_1,s_1,r_1,c,p_2,s_2,r_2\}$. Based on the mathematical model established above, Figure 1(b) can be described by the following formulas:

$$\frac{d\dot\phi_{p_1}}{dt}=\gamma_p^2\left\{-\phi_{p_1}(t)+F\left[V_{p_1}(t)\right]\right\}-2\gamma_p\dot\phi_{p_1}, \tag{2.6}$$

$$\frac{d\dot V_{p_1}}{dt}=\alpha\beta\left\{-V_{p_1}(t)+C_{p_1p_1}\phi_{p_1}(t)-C_{p_1i_1}F\left[V_{i_1}(t)\right]+C_{p_1s_1}F\left[V_{s_1}(t)\right]\right\}-(\alpha+\beta)\dot V_{p_1}(t), \tag{2.7}$$

$$\frac{d\dot V_{s_1}}{dt}=\alpha\beta\left\{-V_{s_1}(t)+C_{s_1p_1}\phi_{p_1}(t)-C_{s_1r_1}^A F\left[V_{r_1}(t)\right]-C_{s_1r_1}^B F\left[V_{r_1}(t-\tau)\right]+P_n\right\}-(\alpha+\beta)\dot V_{s_1}(t), \tag{2.8}$$

$$\frac{d\dot V_{r_1}}{dt}=\alpha\beta\left\{-V_{r_1}(t)+C_{r_1p_1}\phi_{p_1}(t)+C_{r_1s_1}F\left[V_{s_1}(t)\right]+S_{DBS}(t)\right\}-(\alpha+\beta)\dot V_{r_1}(t), \tag{2.9}$$

$$\frac{d\dot V_c}{dt}=\alpha\beta\left\{-V_c(t)+K_1\phi_{p_1}(t)+K_2F\left[V_{s_1}(t)\right]\right\}-(\alpha+\beta)\dot V_c(t), \tag{2.10}$$

$$\frac{d\dot\phi_{p_2}}{dt}=\gamma_p^2\left\{-\phi_{p_2}(t)+F\left[V_{p_2}(t)\right]\right\}-2\gamma_p\dot\phi_{p_2}, \tag{2.11}$$

$$\frac{d\dot V_{p_2}}{dt}=\alpha\beta\left\{\begin{array}{l}-V_{p_2}(t)+C_{p_2p_2}\phi_{p_2}(t)-C_{p_2i_2}F\left[V_{i_2}(t)\right]\\+C_{p_2s_2}F\left[V_{s_2}(t)\right]-K_3F\left[V_c(t)\right]\end{array}\right\}-(\alpha+\beta)\dot V_{p_2}(t), \tag{2.12}$$

$$\frac{d\dot V_{s_2}}{dt}=\alpha\beta\left\{\begin{array}{l}-V_{s_2}(t)+C_{s_2p_2}\phi_{p_2}(t)-C_{s_2r_2}^A F\left[V_{r_2}(t)\right]\\-C_{s_2r_2}^B F\left[V_{r_2}(t-\tau)\right]-K_4F\left[V_c(t)\right]+P_n\end{array}\right\}-(\alpha+\beta)\dot V_{s_2}(t), \tag{2.13}$$

$$\frac{d\dot V_{r_2}}{dt}=\alpha\beta\left\{\begin{array}{l}-V_{r_2}(t)+C_{r_2p_2}\phi_{p_2}(t)\\+C_{r_2s_2}F\left[V_{s_2}(t)\right]-K_5F\left[V_c(t)\right]\end{array}\right\}-(\alpha+\beta)\dot V_{r_2}(t). \tag{2.14}$$

Most of the parameters of formulas (6)–(14) are referenced from [35,36]. These parameters have been shown to apply to previous studies [43–45]. The parameters of this paper are shown in Tables A1 and A2.
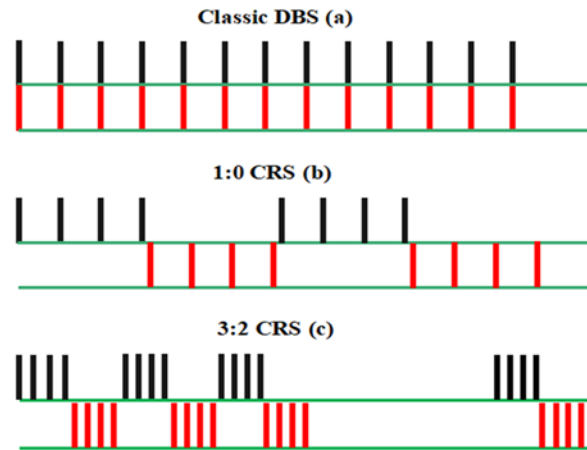
Figure 2. Three different forms of stimulation. (a) Classic DBS. (b) 1:0 CRS. (c) 3:2 CRS.

DBS and CRS are a commonly used in the treatment of epilepsy. We applied DBS, 1:0 CRS and 3:2 CRS to TRN_1 to the model of this paper. The stimulus patterns of DBS, 1:0 CRS and 3:2 CRS are shown in Figure 2(a)–(c), respectively. Here we use a periodic step function to simulate DBS and CRS [14]:

$$S_{DBS}(t) = \rho * H\left(\sin(\frac{2\pi}{T}t)\right)\left(1 - H\left(\sin(\frac{2\pi(t+\delta)}{T})\right)\right),\tag{2.15}$$

$$y(t) = -(\rho * \frac{\left|\sin(2\pi * (t/(8*T)))\right|}{\sin(2\pi * (t/(8*T)))} + \rho)/2,\tag{2.16}$$

$$z(t) = -(\rho * \frac{\left|\sin(2\pi * (t/(40*T)))\right|}{\sin(2\pi * (t/(40*T)))} - \rho)/2,\tag{2.17}$$

$$P = S_{DBS}(t) - y(t) - \rho,\tag{2.18}$$

when $P < 0$, we set $P = 0$, so the expression for 1:0 CRS is

$$S_{1:0CRS}(t) = P,\tag{2.19}$$

$$M = P - z(t),\tag{2.20}$$

if $M < 0$, we set $M = 0$, the expression of 3:2 CRS is

$$S_{3:2CRS} = M,\tag{2.21}$$

where ρ is the amplitude of oscillation. T and δ represent the period and pulse width of the function, we set $\rho = 6$ mV, $\frac{1}{T} = 500$ Hz and $\delta = 1$ ms in this paper. H is Heaviside function in MATLAB.

In addition to the external electrical signals can affect epilepsy, changes in ion concentration inside and outside the cell will produce electromagnetic induction, which can also affect the generation of epilepsy. Under the influence of the electromagnetic induction, we can introduce a memristor to represent the relationship between membrane potential and magnetic flux. The charge flux of the memristor varies as follow [46–48]:

$$\chi(\varphi) = \frac{dc(\varphi)}{dt} = \alpha + 3\beta\varphi^2, \tag{2.22}$$

where $c(\varphi)$ is the flux of charge on the memristor. φ represents the magnetic flux.

A memristor is added to the model in this paper as shown below [32–34]:

$$\frac{d\dot{\phi}_{p_1}}{dt} = \gamma_p^2 \left\{ -\phi_{p_1}(t) + F\left[V_{p1}(t)\right] \right\} - 2\gamma_p \dot{\phi}_{p_1}(t) - w\chi(\varphi)\phi_{p_1}, \tag{2.23}$$

$$\frac{d\varphi}{dt} = w_1\phi_{p_1} - w_2\varphi, \tag{2.24}$$

w is the gain factor association with media, $w_1\phi_{p_1}$ shows the effect of the electromagnetic induction and w_1 has different effects on epilepsy for different mediators. $w_2\varphi$ represents the self inductance effect and also explain the saturation of magnetic flux in the cell. The relevant parameters of the memristor also came from [32]. In this paper, the simulation environment is MATLAB R2019b and we use the forth-order Runge-Kutta method to solve the delay different equation. The total time of the numerical calculation is 15 s and the time step is 0.5 ms.

3. Numerical results

3.1. Generation of epilepsy in the thalamocortical system

Many studies have shown that GABA_B synapses in the thalamus play an important role in suppressing epilepsy in the TRN-SRN pathway, and GABA_B is related to the production of slow waves in the brain. Therefore, adjusting the coupling strength between TRN and SRN may lead to epilepsy [49–51]. In order to verify the validity of the above pathological factors in the model presented in this paper, we applied two related parameters: the inhibitory coupling strength $C_{s_1 r_1}$ and the delay τ of the GABA_B. Figure 3(a) and (b) respectively show the dynamic state analysis and frequency analysis in the parameter space $(C_{s_1 r_1}, \tau)$. The first dynamic state is called the saturation state, where $C_{s_1 r_1}$ is very small. Under this condition, inhibition of TRN_1 and SRN_1 pathways didn't successfully inhibit the over excitation of the cortical thalamic system. At this moment, the firing state of the neuron will quickly evolve from low to maximum, as shown in Figure 3(c). When the values of $C_{s_1 r_1}$ and τ are appropriate, the SWD oscillating state with double peaks is shown in Figure 3(d). More importantly, we find that most SWD oscillations were in the frequency range of 2–4 Hz and the SWDs in these regions were very similar to the EEG signals of patients [3,23]. As the value of $C_{s_1 r_1}$ continues to increase, there will be simple oscillatory state, the simple oscillatory state is shown in Figure 3(e). When the value $C_{s_1 r_1}$ is relatively large, the low discharge state shown in Figure 3(f) will appear. In the paper, we denote saturation, simple oscillation, SWD, and low firing state by I, II, III, and IV, respectively.

The above findings confirm that the model in this paper can reproduce four different dynamic states in the human brain. More importantly, our model can successfully reproduce SWDs with the frequency of 2–4 Hz after introducing the above epileptic pathogenesis. In the next, we will try different coupling interaction and different stimulus methods to explore the pathogenesis of epilepsy.
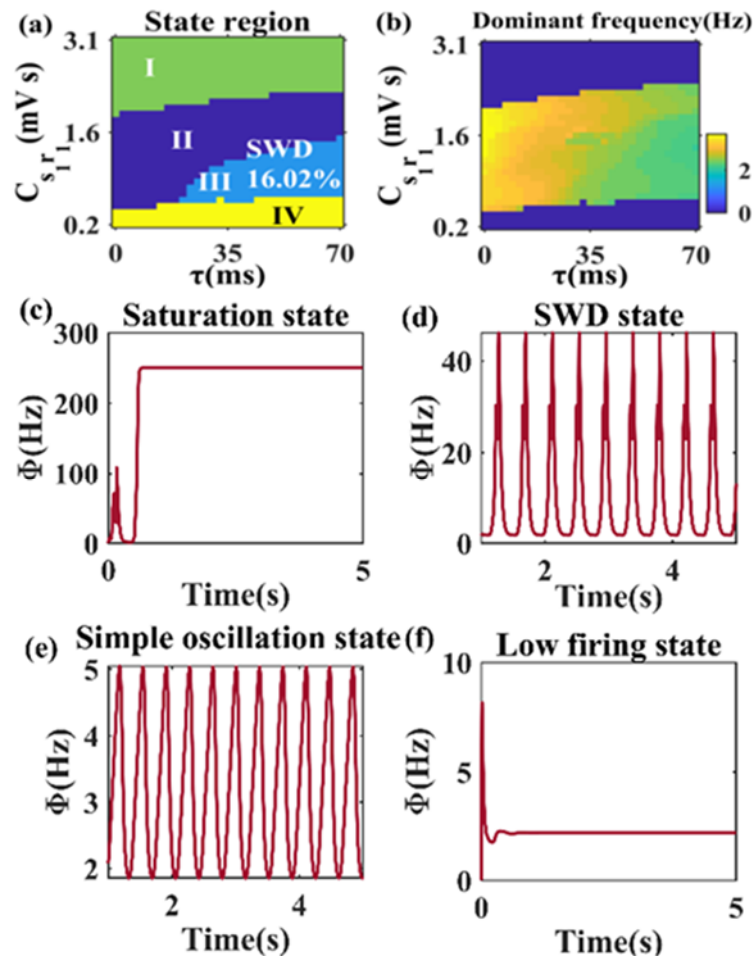
Figure 3. Dynamic analysis in the panel $(C_{s_1 r_1}, \tau)$. (a) State analysis. (b) Frequency analysis. (c) Saturation state (IV). (d) SWD (III). (e) Simple oscillation state (II). (f) Low firing state (I). Here, $\tau = 50$ ms and $C_{s_1 r_1} = 0.5$ mV s (for saturation state), $C_{s_1 r_1} = 1$ mV s (for SWD), $C_{s_1 r_1} = 2$ mV s (for simpleoscillation state) and $C_{s_1 r_1} = 3.1$ mV s (for low firing state), respectively.

3.2. Effects of the TRN₁-SRN₁ pathway on epilepsy control after electrical stimulation and electromagnetic radiation stimulation

Based on Figure 3(a) and (b), electrical stimulation and electromagnetic radiation stimulation are applied to TRN₁ and PY₁ in the model respectively and then we observe the changes in the epileptic region. Electrical stimulation includes DBS, 1:0 CRS and 3:2 CRS, respectively. In addition, we use memristor to simulate the electromagnetic induction changes in the cell body.

As shown in Figure 4(a) and (b), the epileptic area changes from 16.02% in Figure 3(a) to 3.12% after adding DBS. The area of epilepsy is reduced to 8.16% after adding 1:0 CRS shown in Figure 4(c) and (d), 12.82% after adding 3:2 CRS shown in Figure 4(e) and (f), 6.78% after adding electromagnetic radiation shown in Figure 4(g) and (h). These studies have shown that both electrical stimulation and electromagnetic radiation stimulation have inhibitory effects on the production of epilepsy, among which DBS has a better inhibitory effect than 1:0 CRS and 3:2 CRS.
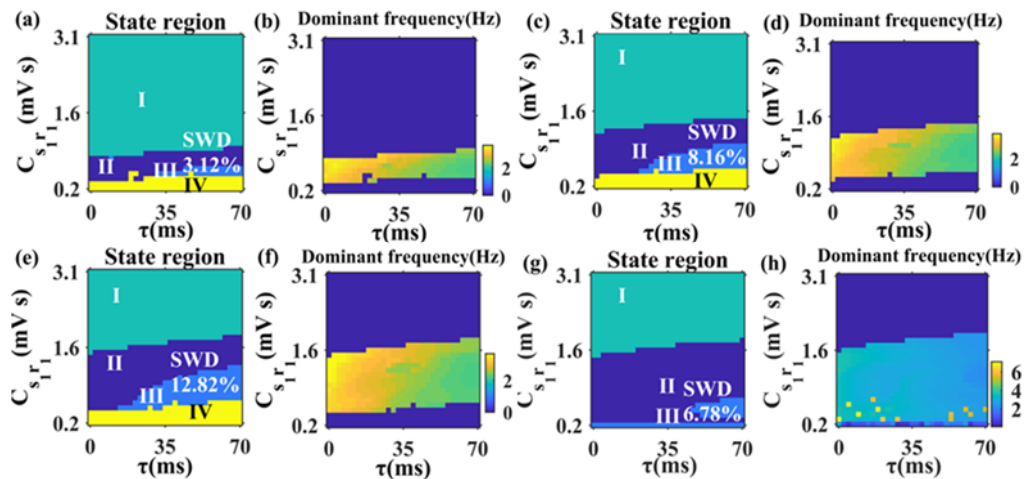
Figure 4. Inhibitive effect of electrical stimulation and electromagnetic radiation. Dynamic and frequency analysis after adding DBS in (a) and (b). 1:0 CRS in (c) and (d). 3:2 CRS in (e) and (f). Memristor in (g) and (h).

3.3. Effects of the TRN$_1$-SRN$_1$ and TRN$_2$-SRN$_2$ pathways interaction on epilepsy after electrical stimulation and electromagnetic radiation stimulation

In addition to exploring the effect of a single pathway and corticothalamic system on epilepsy. Here, we will explore the effect of two pathways belonging to two different corticothalamic systems on epilepsy. We remain applying DBS, 1:0 CRS and 3:2 CRS to TRN$_1$ and electromagnetic radiation stimulation to PY$_1$. Figure 5(a) and (b) shows the dynamic states and dominant frequency analysis of the neurons without any external stimulus, in which the percentage of epileptic area is 25.91%. When we applied DBS to the model, the epileptic area accounts for 10.93% shown in Figure 5(c) and (d). The suppression effect is shown in Figure 5(e)–(h), the epileptic area accounts for 14.05% after adding 1:0 CRS and 21.85% after adding 3:2 CRS, respectively. In addition, the effect of memristor on the dynamic states and dominant frequency of neurons are shown in Figure 5(i) and (j), the epileptic area is significantly reduced compared with Figure 5(a) and (b).

To further explore how to reduce the area of epilepsy, we change the coupling strength between the connector and SRN$_2$. We set K_4 = 0 mV s. On this basis, then we apply electric stimulation and electromagnetic radiation stimulation to the model. In this case, no external stimulation is added as shown in Figure 6(a) and (b), where the epileptic area accounts for 20.92%. When DBS is applied to TRN$_1$, the proportion of epileptic area is 6.76% in Figure 6(c), its dominant frequency analysis is shown in Figure 6(d). We also added 1:0 CRS and 3:2 CRS to the model. As shown in Figure 6(e) and (g), the ratios of epileptic area are 13.22 and 17.59%, respectively. In the dominant frequency analysis diagrams of Figure 6(f) and (h), there are two SWD regions which become smaller than that shown in Figure 6(b). Figure 6(i) and (j) shows the inhibitory effect of the memristor on the cerebral cortex, and the proportion of epileptic area reduced to 11.97%.
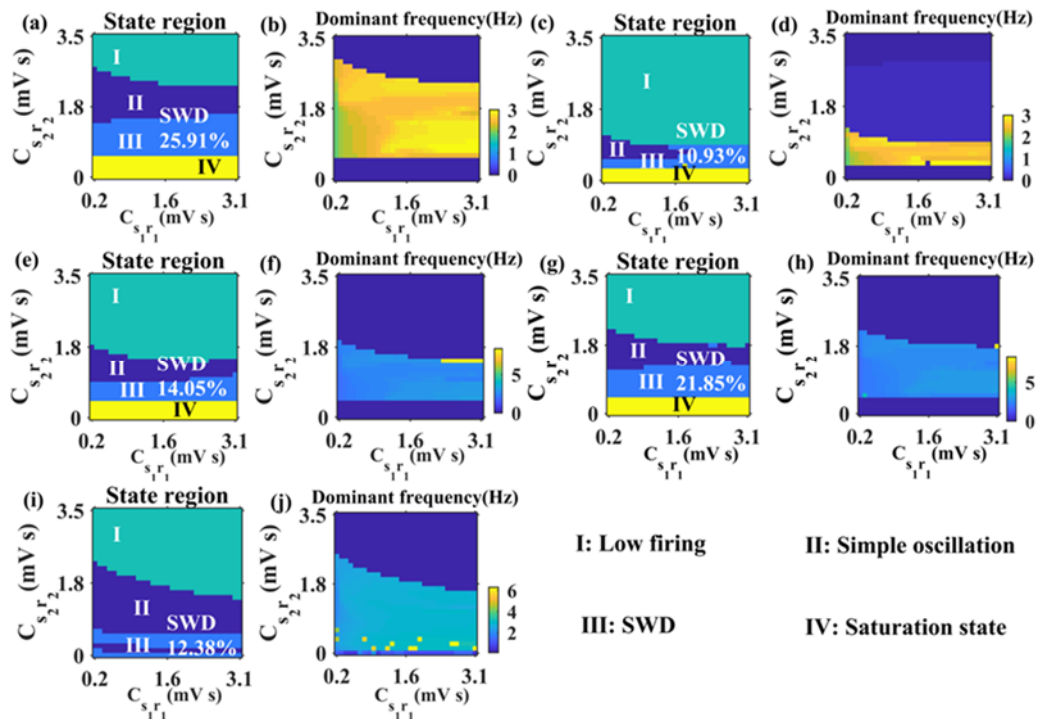
Figure 5. Inhibitive effect of electrical stimulation and electromagnetic radiation in the panel $(C_{s_1 r_1}, C_{s_2 r_2})$. Dynamic states without external stimulation in (a) and (b). After adding DBS in (c) and (d). After adding 1:0 CRS in (e) and (f). After adding 3:2 CRS in (g) and (h). After adding memristor in (i) and (j).

Figure 6. Inhibitive effect of electrical stimulation and electromagnetic radiation in the panel $(C_{s_1 r_1}, C_{s_2 r_2})$ at $K_4 = 0$ mV s. Dynamic states without external stimulation in (a) and (b). After adding DBS in (c) and (d). After adding 1:0 CRS in (e) and (f). After adding 3:2 CRS in (g) and (h). After adding memristor in (i) and (j).
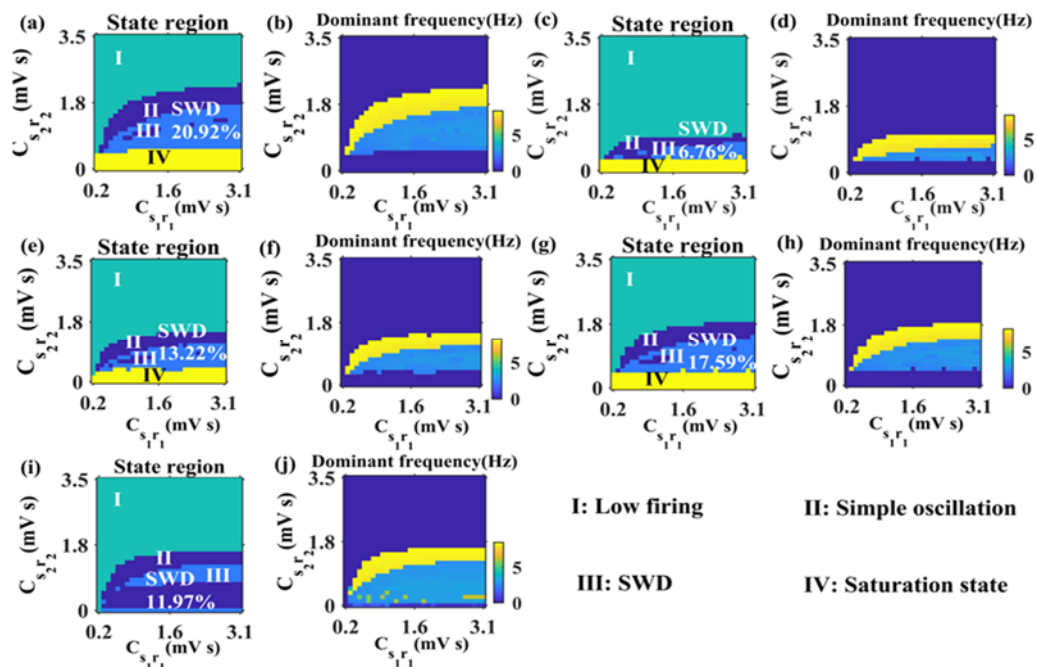
In addition to the above examples, we can also change the coupling strength between the connector and TRN_2 to compare the inhibitory effect of various stimulation methods on epilepsy. In the absence of electrical stimulation and memristor, the dynamic states of neuron and dominant frequency analysis are shown in Figure 7(a) and (b) at $K_5 = 0$ mV s, the SWD oscillation state accounts for 15.50% of the total state. Figure 7(c) and (d) represents the effect of DBS on TRN_1 and the area of epilepsy accounts for 4.68%. The dynamic states and dominant frequency analysis of 1:0 CRS are shown in Figure 7(e) and (f), the percentage of epileptic area is 9.98%. The effect of 3:2 CRS on TRN_1 is shown in Figure 7(g) and (h), and its SWD area occupies 13.84%. When memristor stimulation is applied to PY_1, its inhibitive effect is shown in Figure 7(i) and (j), where the proportion of epileptic area is 0.00%.

In the case of TRN_1-SRN_1 and TRN_2-SRN_2 pathways interaction on epilepsy, comparing the inhibitory effects without external stimulus in Figure 8, we found that epileptic seizure is effectively suppressed by changing the coupling strengths K_4 and K_5, artificially. The $K_5 = 0$ produces a better suppression result than the other approach $K_4 = 0$. With external stimulus, the result shows that numbers of epileptic seizure take on degression after adding DBS, 1:0 CRS, 3:2 CRS and memristor shown in Figure 8. In particular, for optimal effectiveness, the control should be add memristor and set $K_5 = 0$.
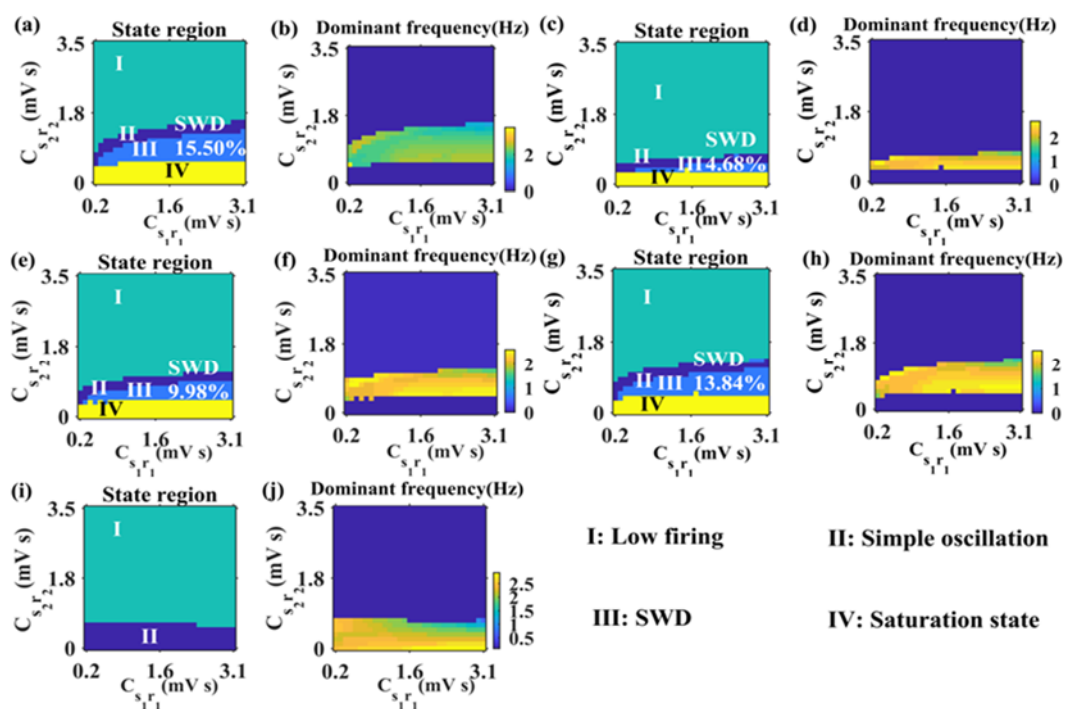

Figure 7. Inhibitive effect of electrical stimulation and electromagnetic radiation in the panel $(C_{s_1 r_1}, C_{s_2 r_2})$ at $K_5 = 0$ mV s. Dynamic states without external stimulation in (a) and (b). After adding DBS in (c) and (d). After adding 1:0 CRS in (e) and (f). After adding 3:2 CRS in (g) and (h). After adding memristor in (i) and (j).
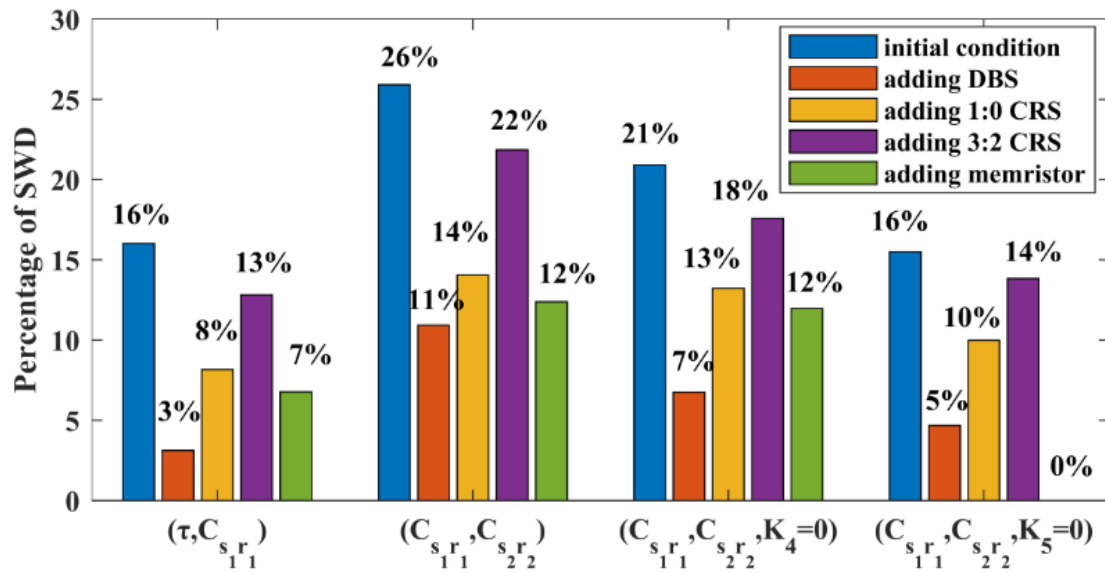
Figure 8. Comparison chart of under different parameter combinations.

4. Conclusions

In the paper, we proposed a novelty model that is composed of two corticothalamic systems and a basal ganglia simplified as a connector. Based on the coupled reduced corticothalamic model, the dynamic state of epileptic seizures was reproduced, and three electrical stimulations and electromagnetic radiation stimulation were added to the model such as DBS, 1:0 CRS and 3:2 CRS. The main findings of the paper are as follows: the complexity of interneuronal iterations can be lessened by simplifying the basal ganglia as a connector. Without external stimulation, the epileptic area can be reduced by changing the coupling strength between the connector and second corticothalamic system. With external stimulation, the results show that DBS has a better effect inhibitory on epilepsy than 1:0 CRS and 3:2 CRS, and 1:0 CRS is better than 3:2 CRS. In addition, the electromagnetic induction from memristor is utilized to suppress epilepsy, and the results show that this method also has a great effect on the suppress epilepsy. This optimal control for electromagnetic induction is confirmed when $K_5 = 0$. These findings have significant implications for the understanding of how to do the theoretical experiment of mean field model for a more simple and convenient method, and how to select external stimulation for suppressing epilepsy. We hope that the numerical simulation results of this paper can provide some insights into the treatment of epileptic patients in clinical therapeutics. In the future work, we will design a closed-loop control method to inhibit epileptic seizure.

Acknowledgments

Conflict of interest

The authors declare there is no conflicts of interest.

References

1. R. M. Durón, M. T. Medina, I. E. Martínez-Juárez, Seizures of idiopathic generalized epilepsies, *Epilepsia*, **46** (2010), 34–47. https://doi.org/10.1111/j.1528-1167.2005.00312.x

2. A. Tolaymat, A. Nayak, J. D. Geyer, Diagnosis and management of childhood epilepsy, *Curr. Probl. Pediatr. Adolesc. Health Care*, **45** (2015), 3–17. https://doi.org/10.1016/j.cppeds.2014.12.002

3. V. Crunelli, N. Leresche, Childhood absence epilepsy: Genes, channels, neurons and networks, *Nat. Rev. Neurosci.*, **3** (2002), 371–382. https://doi.org/10.1038/nrn811

4. R. Guerrini, F. Melani, C. Brancati, A. R. Ferrari, Dysgraphia as a mild expression of dystonia in children with absence epilepsy, *Plos One*, **10** (2015), e0130883. https://doi.org/10.1371/journal.pone.0130883

5. E. Murphy, K. Hoshi, A. Benítez-Burraco, Subcortical syntax: Reconsidering the neural dynamics of language, *J. Neurolinguistics*, **62** (2022), 101062. https://doi.org/10.1016/j.jneuroling.2022.101062

6. G. Leisman, O. Braun-Benjamin, R. Melillo, Cognitive-motor interactions of the basal ganglia in development, *Front. Syst. Neurosci.*, **8** (2014), 16. https://doi.org/10.3389/fnsys.2014.00016

7. C. Marescaux, M. Vergnes, Genetic absence epilepsy in rats from strasbourg (GAERS), *Ital. J. Neurol. Sci.*, **16** (1995), 113–118. https://doi.org/10.1007/BF02229083

8. A. M. L. Coenen, E. L. J. M. Luijtelaar, Genetic animal models for absence epilepsy: A review of the WAG/Rij strain of rats, *Behav. Genet.*, **33** (2003), 635–655. https://doi.org/10.1023/A:1026179013847

9. I. Timofeev, M. Steriade, Neocortical seizures: Initiation, development and cessation, *Neuroscience*, **123** (2004), 299–336. https://doi.org/10.1016/j.neuroscience.2003.08.051

10. R. L. Albin, A. B. Young, J. B. Penney, The functional anatomy of basal ganglia disorders, *Trends Neurosci.*, **12** (1989), 366–375. https://doi.org/10.1016/0166-2236(89)90074-X

11. A. Parent, L. N. Hazrati, Functional anatomy of the basal ganglia. I. The cortico-basal ganglia-thalamo-cortical loop, *Brain Res. Rev.*, **20** (1995), 91–127. https://doi.org/10.1016/0165-0173(94)00007-C

12. D. Pinault, The thalamic reticular nucleus: Structure, function and concept, *Brain Res. Rev.*, **46** (2004), 1–31. https://doi.org/10.1016/j.brainresrev.2004.04.008

13. R. W. Guillery, J. K. Harting, Structure and connections of the thalamic reticular nucleus: Advancing views over half a century, *J. Comp. Neurol.*, **463** (2003), 360–371. https://doi.org/10.1002/cne.10738

14. Z. Wang, Q. Wang, Stimulation strategies for absence seizures: Targeted therapy of the focus in coupled thalamocortical model, *Nonlinear Dyn.*, **96** (2019), 1649–1663. https://doi.org/10.1007/s11071-019-04876-z

15. T. Bessaïh, L. Bourgeais, C. I. Badiu, D. A. Carter, T. I. Toth, Nucleus-specific abnormalities of GABAergic synaptic transmission in a genetic model of absence seizures, *J. Neurophysiol.*, **96** (2006), 3074–3081. https://doi.org/10.1152/jn.00682.2006

16. S. Seo, B. Leitch, Synaptic changes in GABAA receptor expression in the thalamus of the stargazer mouse model of absence epilepsy, *Neuroscience*, **306** (2015), 28–38. https://doi.org/10.1016/j.neuroscience.2015.08.021

17. G. Avanzini, M. D. Curtis, C. Marescaux, F. Panzia, R. Sreafico, M. Vergnes, Role of the thalamic reticular nucleus in the generation of rhythmic thalamo-cortical activities subserving spike and waves, in *Generalized Non-Convulsive Epilepsy: Focus on GABA-B Receptors*, Springer, Vienna, **35** (1992), 85–95. https://doi.org/10.1007/978-3-7091-9206-1_6

18. Z. Nanobashvili, T. Chachua, A. Nanobashvili, I. Bilanishvili, O. Lindvall, Z. Kokaia, Suppression of limbic motor seizures by electrical stimulation in thalamic reticular nucleus, *Exp. Neurol.*, **181** (2003), 224–230. https://doi.org/10.1016/S0014-4886(03)00045-1

19. C. R. Pantoja-Jiménez, V. M. Magdaleno-Madrigal, S. Almazán-Alvarado, R. Fernández-Masa, Anti-epileptogenic effect of high-frequency stimulation in the thalamic reticular nucleus on PTZ-induced seizures, *Brain Stimul.*, **7** (2014), 587–594. https://doi.org/10.1016/j.brs.2014.03.012

20. A. Clemente-Perez, S. R. Makinson, B. Higashikubo, S. Brovarney, Distinct thalamic reticular cell types differentially modulate normal and pathological cortical rhythms, *Cell Rep.*, **19** (2017), 2130–2142. https://doi.org/10.1016/j.celrep.2017.05.044

21. W. J. Chang, W. P. Chang, B. C. Shyu, Suppression of cortical seizures by optic stimulation of the reticular thalamus in PV-mhChR2-YFP BAC transgenic mice, *Mol. Brain*, **10** (2017), 1–15. https://doi.org/10.1186/s13041-017-0320-0

22. P. Kwan, M. J. Brodie, Early identification of refractory epilepsy, *New Engl. J. Med.*, **342** (2000), 314–319. https://doi.org/10.1056/NEJM200002033420503

23. J. Engel, S. Wiebe, J. French, M. Sperling, P. Williamson, D. Spencer, et al., Practice parameter: temporal lobe and localized neocortical resections for epilepsy, *Neurology*, **60** (2003), 538–547. https://doi.org/10.1212/01.WNL.0000055086.35806.2D

24. P. Kwan, S. C. Schachter, M. J. Brodie, Drug-resistant epilepsy, *New Engl. J. Med.*, **365** (2011), 919–926. https://doi.org/10.1056/NEJMra1004418

25. K. Lehtimäki, J. W. Långsjö, J. Ollikainen, H. Heinonen, M. Möttönen, Successful management of super-refractory status epilepticus with thalamic deep brain stimulation, *Ann. Neurol.*, **81** (2017), 142–146. https://doi.org/10.1002/ana.24821

26. I. Adamchic, C. Hauptmann, U. B. Barnikol, N. Pawelczyk, O. Popovych, T. T. Barnikol, Coordinated reset neuromodulation for Parkinson's disease: Proof-of-concept study, *Mov. Disord.*, **29** (2014), 1679–1684. https://doi.org/10.1002/mds.25923

27. D. Fan, Q. Wang, Closed-loop control of absence seizures inspired by feedback modulation of basal ganglia to the corticothalamic circuit, *IEEE Trans. Neural Syst. Rehabil. Eng.*, **28** (2020), 581–590. https://doi.org/10.1109/TNSRE.2020.2969426

28. S. Majhi, D. Ghosh, Alternating chimeras in networks of ephaptically coupled bursting neurons, *Chaos: An Interdiscip. J. Nonlinear Sci.*, **28** (2018), 083113. https://doi.org/10.1063/1.5022612

29. B. K. Bera, S. Rakshit, D. Ghosh, J. Kurths, Spike chimera states and firing regularities in neuronal hypernetworks, *Chaos: An Interdiscip. J. Nonlinear Sci.*, **29** (2019), 053115.

30. S. Rakshit, A. Ray, B. K. Bera, D. Ghosh, Synchronization and firing patterns of coupled Rulkov neuronal map, *Nonlinear Dyn.*, **94** (2018), 785–805. https://doi.org/10.1007/s11071-018-4394-8

31. C. Wang, J. Tang, J. Ma, Minireview on signal exchange between nonlinear circuits and neurons via field coupling, *Eur. Phys. J. Spec. Top.*, **228** (2019), 1907–1924. https://doi.org/10.1140/epjst/e2019-800193-8

32. M. Vinaya, R. P. Ignatius, Electromagnetic radiation from memristor applied to basal ganglia helps in controlling absence seizures, *Nonlinear Dyn.*, **101** (2020), 2369–2380. https://doi.org/10.1007/s11071-020-05955-2

33. M. Lv, J. Ma, Multiple modes of electrical activities in a new neuron model under electromagnetic radiation, *Neurocomputing*, **205** (2016), 375–381. https://doi.org/10.1016/j.neucom.2016.05.004

34. M. Lv, C. Wang, G. Ren, J. Ma, X. Song, Model of electrical activity in a neuron under magnetic flow effect, *Nonlinear Dyn.*, **85** (2016), 1479–1490. https://doi.org/10.1007/s11071-016-2773-6

35. M. Chen, D. Guo, T. Wang, W. Jing, Y. Xia, P. Xu, et al., Bidirectional control of absence seizures by the basal ganglia: A computational evidence, *PLoS Comput. Biol.*, **10** (2014), e1003495. https://doi.org/10.1371/journal.pcbi.1003495

36. M. Chen, D. Guo, M. Li, S. Wu, J. Ma, Y. Cui, et al., Critical roles of the direct GABAergic pallido-cortical pathway in controlling absence seizures, *PLoS Comput. Biol.*, **11** (2015), e1004539. https://doi.org/10.1371/journal.pcbi.1004539

37. P. A. Robinson, C. J. Rennie, D. L. Rowe, Dynamics of large-scale brain activity in normal arousal states and epileptic seizures, *Phys. Rev. E*, **65** (2002), 041924. https://doi.org/10.1103/PhysRevE.65.041924

38. M. Breakspear, J. A. Roberts, J. R. Terry, S. Rodrigues, N. Mahant, P. A. Robinson, A unifying explanation of primary generalized seizures through nonlinear brain modeling and bifurcation analysis, *Cereb. Cortex*, **16** (2006), 1296–1313. https://doi.org/10.1093/cercor/bhj072

39. P. A. Robinson, C. J. Rennie, J. J. Wright, Propagation and stability of waves of electrical activity in the cerebral cortex, *Phys. Rev. E*, **56** (1997), 826–840. https://doi.org/10.1103/PhysRevE.56.826

40. P. A. Robinson, C. J. Rennie, J. J. Wright, H. Bahramali, E. Gordon, D. L. Rowe, Prediction of electroencephalographic spectra from neurophysiology, *Phys. Rev. E*, **63** (2001), 021903. https://doi.org/10.1103/PhysRevE.63.021903

41. S. J. van Albada, R. T. Gray, P. M. Drysdale, P. A. Robinson, Mean-field modeling of the basal ganglia-thalamocortical system. II: Dynamics of parkinsonian oscillations, *J. Theor. Biol.*, **257** (2009), 664–688. https://doi.org/10.1016/j.jtbi.2008.12.013

42. B. Hu, Q. Wang, Controlling absence seizures by deep brain stimulus applied on substantia nigra pars reticulata and cortex, *Chaos, Solitons Fractals*, **80** (2015), 13–23. https://doi.org/10.1016/j.chaos.2015.02.014

43. M. I. Gulcebi, S. Ketenci, R. Linke, H. Hacıoğl, Topographical connections of the substantia nigra pars reticulata to higher-order thalamic nuclei in the rat, *Brain Res. Bull.*, **87** (2012), 312–318. https://doi.org/10.1016/j.brainresbull.2011.11.005

44. G. D. Chiara, M. L. Porceddu, M. Morelli, M. L. Mulas, G. L. Gessa, Evidence for a GABAergic projection from the substantia nigra to the ventromedial thalamus and to the superior colliculus of the rat, *Brain Res.*, **176** (1979), 273–284. https://doi.org/10.1016/0006-8993(79)90983-1

45. P. Suffczynski, S. Kalitzin, F. L. Da Silva, Dynamics of non-convulsive epileptic phenomena modeled by a bistable neuronal network, *Neuroscience*, **126** (2004), 467–484. https://doi.org/10.1016/j.neuroscience.2004.03.014

46. Q. Li, S. Tang, H. Zeng, T. Zhou, On hyperchaos in a small memristive neural network, *Nonlinear Dyn.*, **78** (2014), 1087–1099. https://doi.org/10.1007/s11071-014-1498-7

47. Q. Li, H. Zeng, J. Li, Hyperchaos in a 4D memristive circuit with infinitely many stable equilibria, *Nonlinear Dyn.*, **79** (2015), 2295–2308. https://doi.org/10.1007/s11071-014-1812-4

48. D. Cafagna, G. Grassi, On the simplest fractional-order memristor-based chaotic system, *Nonlinear Dynam.*, **70** (2012), 1185–1197. https://doi.org/10.1007/s11071-012-0522-z

49. F. Marten, S. Rodrigues, O. Benjamin, M. P. Richardson, J. R. Terry, Onset of polyspike complexes in a mean-field model of human electroencephalography and its application to absence epilepsy, *Philos. Trans. R. Soc. A*, **367** (2009), 1145–1161. https://doi.org/10.1098/rsta.2008.0255

50. R. L. Macdonald, J. Q. Kang, M. J. Gallagher, H. J. Feng, GABAA receptor mutations epilepsy associated with generalized epilepsies, *Adv. Pharmacol.*, **54** (2006), 147–169. https://doi.org/10.1016/S1054-3589(06)54007-4

51. A. Destexhe, Spike-and-wave oscillations based on the properties of GABAB receptors, *J. Neurosci.*, **18** (1998), 9099–9111. https://doi.org/10.1523/JNEUROSCI.18-21-09099.1998

Appendix

The following parameters are used to numerical simulations [35,36].

Table A1. Default parameters.

Parameters	Meaning	Value
$Q_{p_1,p_2}^{\max}, Q_{i_1,i_2}^{\max}$	Cortical maximum firing rate	250 Hz
$Q_{s_1,s_2}^{\max}$	SRN maximum firing rate	250 Hz
$Q_{r_1,r_2}^{\max}$	TRN maximum firing rate	250 Hz
$Q_c^{\max}$	Connector maximum firing rate	250 Hz
θ_{i_1,i_2}	Mean firing rate threshold of cortical	15 mV
θ_{s_1,s_2}	Mean firing rate threshold of SRN	15 mV
θ_{r_1,r_2}	Mean firing rate threshold of TRN	15 mV
θ_c	Mean firing rate threshold of Connector	10 mV
γ_p	Cortical damping rate	100 Hz
τ	Delay time	50 ms
α	Synaptodendritic decay time constant	50 s^{-1}
β	Synaptodendritic rise time constant	200 s^{-1}
σ	Threshold variability of firing rate	6 mV
P_n	Nonspecific input	2 mV s

Table A2. Strength of coupling.

Parameters	Source	Target	Value
$C_{p_1 p_1}$	PY$_1$	PY$_1$	1 mV s
$C_{p_1 i_1}$	IN$_1$	PY$_1$	1.8 mV s
$C_{r_1 p_1}$	PY$_1$	TRN$_1$	0.05 mV s
$C_{r_1 s_1}$	SRN$_1$	TRN$_1$	0.5 mV s
$C_{s_1 p_1}$	PY$_1$	SRN$_1$	2.2 mV s
$C_{s_1 r_1}^{A,B}$	TRN$_1$	SRN$_1$	0.8 mV s
$C_{p_1 s_1}$	SRN$_1$	PY$_1$	1.8 mV s
$C_{p_2 p_2}$	PY$_2$	PY$_2$	1 mV s
$C_{p_2 i_2}$	IN$_2$	PY$_2$	1.8 mV s
$C_{r_2 p_2}$	PY$_2$	TRN$_2$	0.05 mV s
$C_{r_2 s_2}$	SRN$_2$	TRN$_2$	0.5 mV s
$C_{s_2 p_2}$	PY$_2$	SRN$_2$	2.2 mV s

Parameters	Source	Target	Value
$C_{s_2 r_2}^{A,B}$	TRN$_2$	SRN$_2$	0.8 mV s
$C_{p_2 s_2}$	SRN$_2$	PY$_2$	1.8 mV s
K_1	PY$_1$	Connector	1 mV s
K_2	SRN$_1$	Connector	0.1 mV s
K_3	Connector	PY$_2$	0.08 mV s
K_4	Connector	SRN$_2$	0.035 mV s
K_5	Connector	TRN$_2$	0.035 mV s